

Classification of Buckling Behavior on Uniaxial Compression using A5052-O Sheets

S.Onoda, S.Yoshihara, B.J.MacDonald and Y.Okude

Abstract—Aluminum alloy sheets have several advantages such as the lightweight, high-specific strength and recycling efficiency. Therefore, aluminum alloy sheets in sheet forming have been used in various areas as automotive components and so forth. During the process of sheet forming, wrinkling which is caused by compression stress might occur and the formability of sheets was affected by occurrence of wrinkling. A few studies of uniaxial compressive test by using square tubes, pipes and sheets were carried out to clarify the each wrinkling behavior. However, on uniaxial compressive test, deformation behavior of the sheets hasn't be cleared. Then, it is necessary to clarify the relationship between the buckling behavior and the forming conditions. In this study, the effect of dimension of the sheet in the buckling behavior on compression test of aluminum alloy sheet was cleared by experiment and FEA. As the results, the buckling deformation was classified by three modes in terms of the distribution of equivalent plastic strain.

Keywords—Sheet forming, Compression test, Aluminum alloy sheet, Buckling behavior

I. INTRODUCTION

ALUMINUM alloy sheets have the characteristics of having lightweight, high-specific strength and high-formability. From these advantages, they have been utilized in various areas after secondary process such as the bending process or deep-drawing process and so forth [1, 2]. In these forming processes, it is important to indicate the occurrence of undesirable deformation, because the forming limit of aluminum alloy sheets was affected by the undesirable deformation. Especially, buckling and wrinkling caused by compression stress are the major defect on sheets forming process in order to be easily occurred buckling and wrinkling. However, these undesirable deformations behavior were made clear even simply forming process as a uniaxial compressive test. Thus, wrinkling was controlled in experimental condition

S.Onoda is with the Department of Mechanical System Engineering, University of Yamanashi., Yamanashi, 4-3-11 Takeda Kofu-city, Japan (phone: +81-55-220-8438; fax: +81-55-220-8779; e-mail: g11mm009@yamanashi.ac.jp).

S. Yoshihara is with the Department of Mechanical System Engineering, University of Yamanashi., Yamanashi, 4-3-11 Takeda Kofu-city, Japan (phone: +81-55-220-8438; fax: +81-55-220-8779; e-mail: yoshihara@yamanashi.ac.jp).

B. J. MacDonald is with the School of Mechanical Engineering, Dublin City University, Dublin 9, Ireland (phone: +353-1-700-8046; fax: +353-1-700-5345; e-mail: bryan.macdonald@dcu.ie).

Y. Okude is with the Engineering for Functional Material System, University of Yamanashi, Yamanashi, 4-3-11 Takeda Kofu-city, Japan (phone: +81-55-220-8438; fax: +81-55-220-8779; e-mail: g10df004@yamanashi.ac.jp).

practically. In order to control wrinkling in theoretical method, the resolving mechanical conditions of buckling behavior in several conditions should be needed. In this study, the buckling caused by compression was focused on using aluminum alloy sheets. The buckling behavior differs from these material properties, the shape of the workpiece, the workpieces dimension, the constraint condition of them and forming speed. Therefore, there are a lot of studies of sheet buckling in elastic range since the application of Timoshenko's beam theory which is absolutely known as the basic theory of buckling. However, these studies have little advantage in real, because the actual deformation is carried out in not only the elastic range but also the plastic range. Therefore, from the practical advantages, there are more studies of buckling behavior in plastic range than the studies of buckling behavior in elastic range until now. The almost studies of sheet buckling in plastic range were carried out from two main objectives. One of them is to calculate the buckling load exactly on compression by several methods such as FEA or elementary analysis. For example, there are the studies which were explained for the buckling load on the difference of the boundary conditions [3], the buckling under compressing were complicated for the dimensions such as ribbed sheet [3-6] and the buckling under compressing special material [6]. Also, the method calculated for the buckling load in the plate on the compression load was developed and modified [7-11]. Another objective is to clear the buckling behavior and the buckling condition in plastic range as the compressed sheet differs from the dimension in several conditions. In common with the study for buckling load, the factors, which influenced buckling behavior such as the material shape and material properties, were investigated by various methods [12-18]. Especially, the study of the buckling behavior when the sheet is compressive in various dimensions is needed. This reason is that the characteristics of the sheet influence the buckling behavior because of the boundary condition of the workpiece. However, the effect of the sheet dimension on the buckling behavior in plastic range wasn't cleared. The dimension of the sheet is the most important factor on the buckling since the dimension of the sheet was depended on the characteristics which mean shape, and buckling behavior. These differences aren't defined and, the sheet dimension decides that buckling is occurred in the elastic range or the plastic range. Therefore, the effect of the sheet dimension on buckling behavior should be needed in order to control wrinkling.

The objective of this study is to clarify the buckling behavior of the aluminum alloy sheet on the compression stress and to classify the difference mode of the buckling behavior of the sheet by using finite element analysis (FEA). In this study, we indicate that the sheet buckling is caused by the compression

stress which was defined as occurring at the maximum compressive load. Additionally, the experiments on the uniaxial compression test were carried out in order to prove the validity of the FEA result. In these results, the buckling behavior was classified into three modes depending on the distribution of the equivalent plastic strain in the buckling of the sheet. These modes which were summarized have characteristic each other and the deformation behavior of the sheet under the uniaxial compression.

II. FEA ON UNIAXIAL COMPRESSIVE TEST UNDER CONSTRAINING CONDITION AT ENDS OF A5052-O SHEET

A. FEA Model and Condition

LS-DYNA was used as the finite element analysis (FEA) code in this study. FEA is utilized in order to simulate the compression process based on the *n*- power law as shown in Eq.1.

$$\sigma = C(\epsilon_e + \epsilon_p)^n \tag{1}$$

where, ϵ_e is the elastic strain at yield point and ϵ_p the effective plastic strain. These jigs and A5052-O sheet were modeled as solid elements. Table I shows the material properties of A5052-O. *C* means strength coefficient and *n* hardening coefficient. Fig.1 shows the schematic of the workpiece and the FEA model in the uniaxial compression test. The rectangular sheet was compressed on the compressive load by the upper jig on constant compressive speed. The uniaxial compression test was carried out under of fixing at both ends and free at both sides of the sheet as the constraint conditions. The workpiece of the sheet was compressed on the compressive rate =5.0(%). Compressive rate is as shown in Eq.2.

$$C_R = \frac{l}{D_c} \times 100(\%) \tag{2}$$

where, D_c is compressive displacement and C_R compressive rate. The friction coefficient between the workpiece and the jigs was set on 0.01. Table II shows the condition of the sheet dimension in FEA. The conditions of the sheet as the difference of the sheet thickness *t* shape were defined as shown in Table II. Sheet length and width were indicated in dimensionless parameter *l/t* and *w/t* to divide by the sheet thickness as shown in Table II.

B. FEA Results

Three types classification of the buckling depending on the distribution equivalent plastic strain in buckling

Table III summarizes the classified three modes of the sheet buckling and indicates the equivalent plastic strain distribution in maximum compressive load in $C_R=5.0(\%)$. These modes were classified in terms of the distribution equivalent plastic strain at the maximum compressive load. The equivalent plastic strain distribution is different on each mode with maintaining the compressive load after the buckling. The range of the equivalent plastic strain in $C_R=5.0(\%)$ as shown in Table III was little due to approaching the border of elastic strain area and plastic strain area. The difference of the equivalent plastic strain distribution was explained that the buckling behavior in terms of growing buckling was difference on each condition.

Table IV shows the schematic of the sheet in the maximum compressive load on the three modes and compressive load – compressive rate curves.

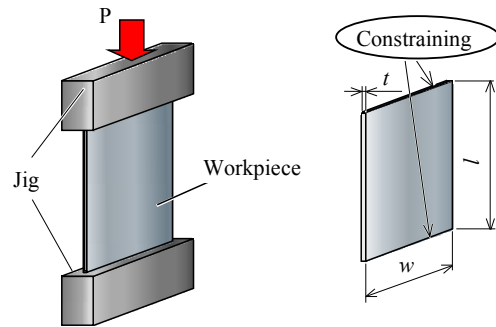


Fig. 1 FEA model and the schematic of workpiece of the uniaxial compression test

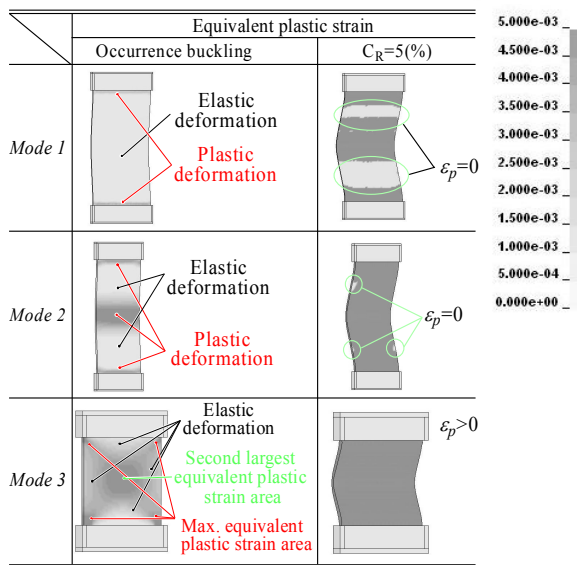
TABLE I
MATERIAL PROPERTY OF A5052-O

Density ρ (10^3kg/m^3)	Modulus of elasticity <i>E</i> (Gpa)	<i>C</i> value (Mpa)	<i>n</i> value
2.68	69.3	515.8	0.33

TABLE II
SHAPE OF SHEET IN FEA

Sheet thickness <i>t</i> (mm)	<i>l/t</i>	<i>w/t</i>
0.5	40, 60, 140, 200	5, 10, 20, 40, 60, 80
1.0	20, 40, 70, 100	5, 10, 20, 40
1.5	10, 20, 35, 70	5, 10, 20
2.0	10, 20, 35, 50	5, 10, 20

TABLE III
THREE MODE CLASSIFICATION OF SHEET BUCKLING DEPENDING ON THE DISTRIBUTION EQUIVALENT PLASTIC STRAIN IN BUCKLING



In this table, the compressive load was expressed in dimensionless parameter σ_t to be divided by the tensile strength. At the beginning of the compression test, the sheet proof the compressive load and the buckling was occurred to be more compressed at the maximum compressive load. After this behavior, the compressive load was decreased by the small expansion of the buckling.

Mode 1- Mode 1 was defined that the plastic strain area was concentrated at the end of the sheet and the elastic buckling area at the nearly middle of the sheet in the buckling. The area which was concentrated the plastic strain was the tiny area by the compression stress in the elastic range area. At $C_R=5.0(\%)$, the buckling in the plastic range was also concentrated at the middle of the sheet into stripes parallel to the constrained side. The plastic strain areas at the end of sheet were increased, and there were the elastic strain areas at between middle and end of the sheet. At the buckling, there was small deflection at the middle of the sheet. Additionally, the sheet had two flexion points at the both ends. Because the sheet was bent with the constrain area and undergo the deflection in the area near middle. Therefore, this point, which was the maximum buckling depth, was not constantly in the middle of the sheet. The flexural deformation area has been progressed the bending deformation by more compression. σ_t was substantially increased and exhibited as linear increase to the maximum σ_t at start compression test. After the buckling, σ_t decreased rapidly and approached to $\sigma_t=0$ slowly.

Mode 2- Mode 2 means that the sheet has had the high equivalent plastic strain into parallel to the constrained side at the middle and the end of the sheet. The equivalent plastic strain area at the middle of the sheet progressively increased from the center outward of the sheet, and the equivalent plastic strain area at the end increased from corner toward the center. The area which was occurring equivalent plastic strain in the middle was larger than the area at the end. Additionally, in comparison with the Mode 1, the area of the equivalent plastic strain at the end of the sheet was large comparatively. The sheet almost has the buckling in the plastic range at $C_R=5.0(\%)$ and there were a little elastic area partially. In Mode 2, the buckling, which was occurred, has had the flexion point since starting buckling. Thus, the buckling behavior was the dogleg shape with the bending at the middle of the sheet due to the start of the buckling.

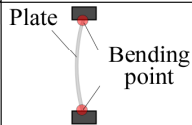
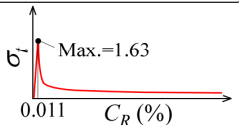
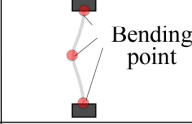
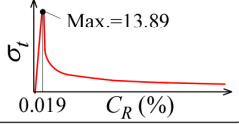
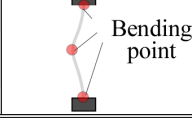
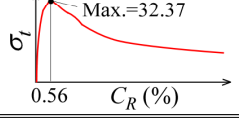
Then, the point was the maximum buckling depth at the middle of the sheet due to occurring the buckling. σ_t-C_R curve in Mode 2 is similar to the Mode 1. However, P/P_t in Mode 2 was eight times as large as Mode 1.

Mode 3- Mode 3 was defined that the area on the kitty-cornered sheet was distributed as the equivalent plastic strain before the buckling. The other area was the elastic range area. The equivalent plastic strain, which was the maximum value at the near corner of the sheet before the buckling, wasn't occurred in nearly middle of each side. At the other area, the equivalent plastic strain concentrated which was small. In common with Mode 2, the sheet in the case of Mode 3 has two flexion points and three bending points at starting the buckling.

Increasing rate of σ_t in Mode 3 is smaller than Mode 1 and 2. Thus, σ_t at the maximum compressive load was twenty times higher than Mode 1. Because the large strain energy was caused by compressive load was stored in the sheet. It is proved that C_R and σ_t of Mode 3 is bigger than Mode 1 and Mode 2.

From these results, it was proved that the sheet dimension effects the classification of the buckling mode depending on the distribution equivalent plastic strain in buckling. Additionally, the extent of the plastic range area was difference by the buckling mode at $C_R=5.0(\%)$ as shown in Table III.

TABLE IV
BEHAVIOR OF THE SHEET IN BUCKLING

	Buckling behavior	The compressive load
Mode 1		
Mode 2		
Mode 3		

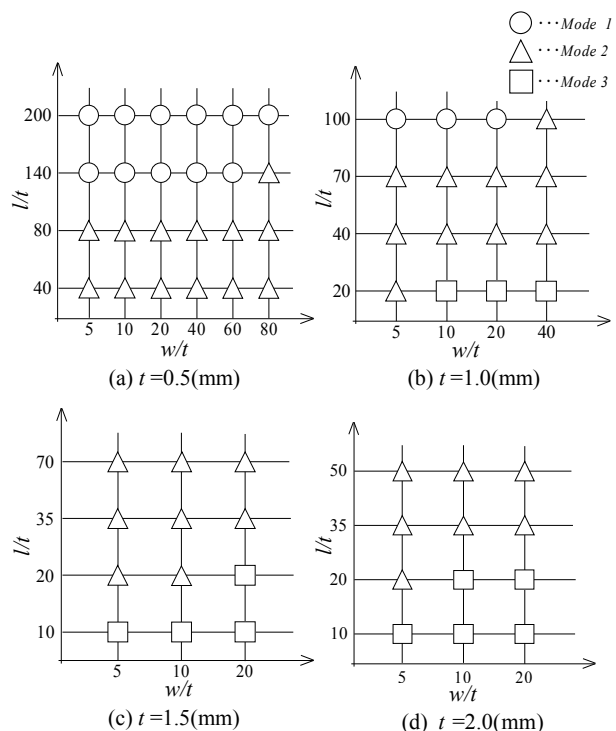


Fig. 2 The effect of sheet dimension on buckling mode classification

Effect of the sheet dimension on the difference of the buckling mode

These differences of the buckling phenomenon were caused by the sheet dimension. Fig.2 shows the effect of sheet dimension on buckling mode classification. The symbol \bigcirc indicates Mode 1, \triangle Mode 2 and \square Mode 3. Sheet length, sheet width and sheet thickness influence the buckling mode independently without effect of the cross section area. For example, the buckling mode on $l/t=40$, $w/t=80$ and $t=0.5(\text{mm})$ was same as on $l/t=20$, $w/t=20$ and $t=1.0(\text{mm})$ in spite of same cross section area. In a similar method, the buckling mode wasn't necessarily to be same in same width-thickness ratio. The buckling mode, when sheet thickness and sheet width were large, and sheet length was small, tended to become Mode 3. On the contrary, the buckling mode is inclined to belong to Mode 1, when sheet has thin thickness, small width and were large length. On the sheet dimension between being Mode 1 and being Mode 3, the buckling mode was also inclined to belong to Mode 2.

Fig.3 shows the effect of the sheet dimension on the compressive rate in the maximum compressive load by the conditions of the difference sheet thickness. The compressive rate in the maximum compressive load would be high as the sheet thickness increases, because of the principal moment of inertia of area as shown in Fig. 4. The compressive rate in the maximum compressive load on $t=1.5(\text{mm})$ and $2.0(\text{mm})$ was much higher than the load on $t=0.5(\text{mm})$ or $1.0(\text{mm})$. The compressive rate in the maximum compressive would be low as l/t is increases. However, the influence of the sheet width on the compressive rate in the buckling was smaller than the case of the sheet length and sheet thickness. Because, the sheet was only bend in the sheet thickness direction. Thus, the sheet length and the sheet thickness were much influenced on the buckling mode because of increasing of the bending moment and the direction in bending.

In comparing Fig.2 with Fig.3, it shows that the buckling mode was concerned with compressive rate in the buckling. The compressive rate in the buckling in the case of Mode 3 was much larger than Mode 1 and Mode 2. Especially, the compressive rate in the buckling in the case of Mode 3 on $t=2.0(\text{mm})$ was ten times larger than the other modes. From these results, the effect of the sheet dimension on difference of the buckling mode was confirmed.

The buckling behavior in terms of position of maximum equivalent plastic strain area by buckling mode

Table V shows the area which was the maximum the equivalent plastic strain in the buckling and $C_R=5.0(\%)$. In this study, there were three areas in which the equivalent plastic strain concentrated and the maximum equivalent plastic strain area differed by the compressive rate. First, Plane O and the Plane I are defined in order to show the maximum equivalent plastic strain area. The plane of the outer surface area with curvature is defined as Plane O and the inner surface as Plane I as shown in Table V. Second, Area a was defined as the area which was surface of Plane I at the center of the sheet, Area b the surface of Plane O at the neighbor side of Area a and Area c

the area of the surface of Plane I in the nearly both the constrained area on the constrained side parallel. In this study, the bending deformation was occurred in the middle of the sheet and nearly both the constrained areas. The equivalent plastic strain in these areas became larger than the other areas. In all mode, Area a is the biaxial state of the tensile stress and Area b is the biaxial state of the compressive stress. Additionally, the stress state of Area c was the compressive stress along the axial direction.

Mode 1- The maximum equivalent plastic strain area was Area c at the buckling. The stress along the axial direction on Area c was larger than other areas. In $C_R=5.0(\%)$, the equivalent plastic strain on Area b was much larger than Area c. Furthermore, the shear stress on area c increased in $C_R=5.0(\%)$.

Mode 2- Unlike on the case of Mode 1, the equivalent plastic strain in the case of Mode 2 was concentrated at Area a at the buckling. The tensile stress along the width direction on Area a was large. As the sheet was compressed, the maximum equivalent plastic strain area was moved at Area b. In common with Mode 1, the shear stress on Area c also increased in $C_R=5.0(\%)$.

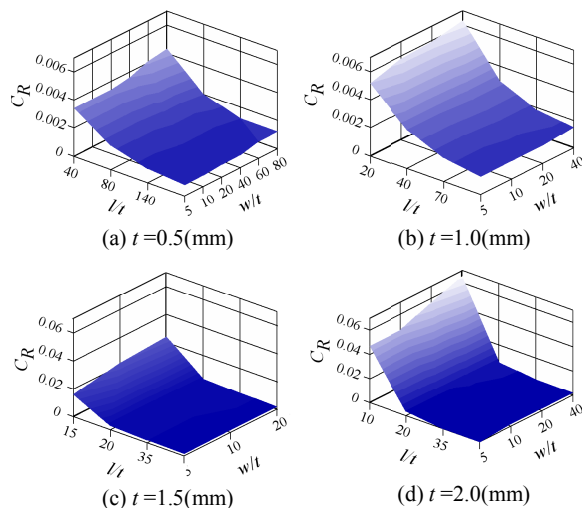
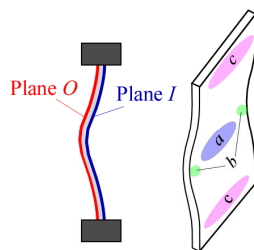


Fig. 3 The effect of sheet dimension on compressive rate in max compressive load

TABLE V
THE MAX EQUIVALENT PLASTIC STRAIN AREA IN MAX COMPRESSIVE LOAD AND $C_R=5.0(\%)$

	Max equivalent plastic strain area	
	Max compressive load	$C_R=5.0(\%)$
Mode 1	c	b
Mode 2	a	b
Mode 3	a	a



Mode 3- The maximum equivalent plastic strain area in the case of Mode 3 was also concentrated at Area *c* like Mode 2. The tensile stress along the width direction on Area *a* also was large. However, unlike the case of mode 2, the maximum equivalent plastic strain area was remained Area *a* at $C_R = 5.0(\%)$. The tensile stress along the width direction on Area *a* was larger than other Area *a* at $C_R = 5.0(\%)$ because the shear stress on Area *a* increased slightly.

Almost sheets, which is same length came into same the figuration like the dogleg shape at $C_R = 5.0(\%)$ although the compressive rate in the buckling is difference. Moreover, despite becoming the same the shape of sheet at $C_R = 5.0(\%)$, the area, which was concentrated the equivalent plastic strain, was divided by the buckling mode. The maximum equivalent plastic strain area moved little by little with the compression of the sheet. Thus, the part of the sheet easily deformed was difference because of the maximum equivalent plastic strain area. The area, which has to be constrained by the jig, was divided by the compressive rate and the buckling mode owing to the difference of the maximum equivalent plastic strain area.

III. EXPERIMENT

A. Experimental condition

The experiment of the compression test was actually carried out. Furthermore, the FEA results were compared with the experiment results in order to validate of it. The effect of the sheet dimension on the springback was confirmed. In addition, in common with the constraining condition of the FEA simulation, the both ends of the sheet were constrained and the side of the sheet was set on the free in the experiment. The testing speed in the compression test was set on 10(mm/min) and the sheet pressed at a constant speed.

B. Springback

The springback r_θ was indicated on dimensionless parameter as shown in Eq.3.

$$r_\theta = \frac{\theta_b - \theta_a}{\theta_a} \times 100 (\%) \tag{3}$$

where θ_a is the angle in the middle of the sheet before unloading and θ_b the angle in the middle of the plate after unloading. These angles measured are the plane of the inner surface area with curvature at $C_R = 5.0(\%)$.

C. Experimental result

Validation of the FEA results by comparing the FEA results with the experimental results

Fig.4 shows the comparison with experimental result and the FEA result in terms of the shape of the sheet and the maximum stress area. Von Mises stress of the stress distribution as showed in Fig.4 indicated. The experimental result was compared with the FEA result on $t=0.5(\text{mm})$, $l/t=140$ and $w/t=80$. The distance of the maximum buckling depth to bottom end on the experiment and one on FEA were 32.9(mm) and 33.6(mm). The buckling depth in the experimental result was 10.3(mm) on the plane of the inner surface area with curvature.

On the other hand, the distance of the maximum buckling depth to above end on the experiment and one on FEA were 33.2(mm) and 33.3(mm). The buckling depth of the FEA result agreed with the experimental result. Furthermore, the point the most deformed was concentrated on Von Mises stress. This position was same as the position of the maximum buckling depth. On the contrary, in the area between the middle of the sheet and the constrain area, the Von Mises stress wasn't concentrated by comparison with other area. Thus, only this area was in elastic range.

From these results, the sheet in FEA is similar to the shape of the experimental result. Then we confirmed that the FEA result is validated by the experimental results.

The effect of the sheet dimension on springback

Fig.5 shows the effect of the sheet dimension on the springback. The sheet width has the small effect on the springback in comparison with the sheet length and the sheet width. In addition, the springback increased as the sheet length increased and the sheet thickness decreased.

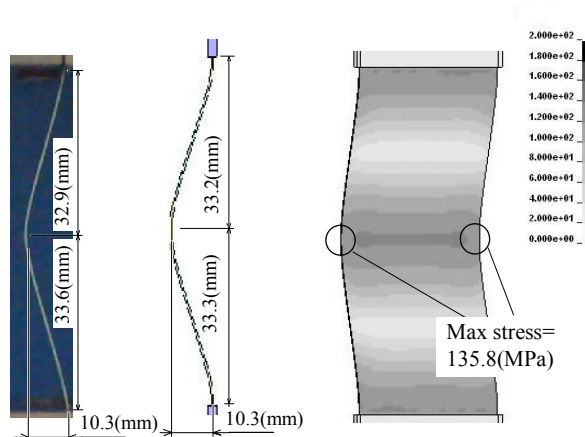


Fig. 4 Comparison FEA results with experimental results

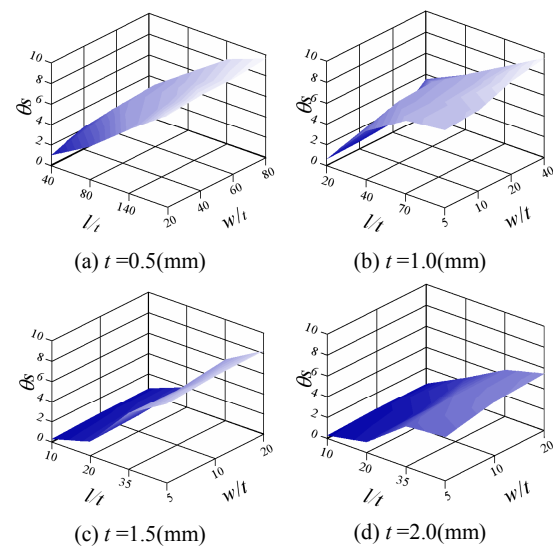


Fig. 5 The effect of dimension on springback

The sheet length strongly affected the springback. For instance, the springback in $t=0.5(\text{mm})$ was larger than the other thickness conditions. Thus, the springback was large when the buckling mode was Mode 1 or Mode 2 because there was the area concentrated elastic strain as shown Fig.2. In Mode 3, the springback was extremely small. This reason is that all around sheet in case of the Mode 3 was the area concentrated the equivalent plastic strain. Furthermore, Fig.5 (a) indicates that in Mode 1 and Mode 2, the tendency of increasing the springback was same.

The springback was difference by the buckling mode. Thus, the sheet in the case of Mode 3 was apply the jig in order to control the buckling.

IV. CONCLUSION

This study indicated that the buckling mode was defined by the equivalent plastic strain distribution and stress in buckling. From these results, these modes have some characteristics for the deformation behavior in forming process by using aluminum alloy sheets.

Mode 1- Mode 1 was defined that the plastic strain area was concentrated at the end of the sheet and the elastic buckling area at the nearly middle in the buckling. In that case, the compressive rate at the buckling was low and, the springback was large. For instance, the compressive rate at the buckling was 0.0012(%) and the springback was 9.8(%) in $t=0.5(\text{mm})$ $l/t=200$ and $w/t=5$. Moreover, when the buckling is controlled partially, the local buckling is occurred in other part because the sheet in Mode1 partially has the large elastic range. The long sheet on the compression test has to be constrained by the jigs all around the material at the end of them. Therefore, controlling buckling in this mode would be difficult.

Mode 2- Mode 2 means that the sheet has had the high equivalent plastic strain into parallel to the constrained side at the middle and the end of the sheet. The compressive rate in the buckling was higher and the springback was larger than Mode 1. The jig to control buckling can be locally applied because the size of the area is the elastic range.

Mode 3- Mode 3 was defined that the area on the kitty-cornered sheet was distributed as the equivalent plastic strain before the buckling. In this mode, the compressive rate in the buckling was high and the springback was small. For example, the compressive rate at the buckling was 0.068(%) and the springback was a little occurred in $t=1.5(\text{mm})$ $l/t=10$, and $w/t=20$. Therefore, to control buckling in this mode would be easy.

The buckling mode applies to some sheet forming processing methods in which the buckling caused on the compressive load occurs. Moreover, this study should be worked to control of the wrinkling during the process. Especially, the processing method which is controlled to wrinkling by using the core bar such as the bending process applies this mechanical condition. In order to control wrinkling, the wrinkling behavior would be needed to be clarified. In this study, the buckling behavior was classified in terms of the equivalent plastic strain. Moreover, the buckling behavior was cleared by this difference conditions of the sheet dimension investigated. Three kinds of the

buckling modes, which were classified by the equivalent plastic strain distribution, have the characteristics of deformation in terms of the shape respectively. In the future, the effect of dimension on the wrinkling behavior should be investigated in order to control wrinkling in the elementary theory. This study has theoretically led to control the mechanism of the wrinkling behavior.

REFERENCES

- [1] M. Kadkhodayan and F. Moayyedean, "Analytical elastic-plastic study on flange wrinkling in deep drawing process," *Scientia Iranica, Mechanical Engineering*, vol.18, Jan, 2011, pp.250-260
- [2] G.Y. Zhao, Y.L. Liu and C.S. Dong, "Analysis of wrinkling limit of rotary-draw bending process for thin-walled rectangular tube," *Journal of Materials Processing Technology*, vol.210, Mar, 2010, pp.1224-1231
- [3] Christian Mittelstedt, "Closed-form analysis of the buckling loads of uniaxially loaded blade-stringer-stiffened composite sheets considering periodic boundary conditions," *Thin-Walled Structures*, vol.45, Apr, 2007, pp.371-382
- [4] Umut Topal and Umit Uzman, "Optimum design of laminated composite sheets to maximize buckling load using MFD method," *Thin-Walled Structures*, vol.45 Aug, 2007, pp. 660-669
- [5] Hongzhi Zhong and Chao Gu, "Buckling of symmetrical cross-ply composite rectangular sheets," *Composite Structure*, vol.80, Apr, 2006, pp. 42-48
- [6] Makarand G.Joshi and Sherrill B. Biggers, Jr, "Thickness optimization for maximum buckling loads in composite laminated sheet," *Composites part*, vol.27, Jun, 1995, pp.105-114
- [7] Y.G. Liu and M.N. Pavlović, "A generalized analytical approach to the buckling of simply-supported rectangular sheets under arbitrary loads," *Engineering structure*, vol. 30, Jul, 2007, pp. 1346-1359
- [8] Xinwei Wang, Xinfeng Wang and Xudong Shi, "Accurate buckling loads of thin rectangular sheets under parabolic edge compressions by the differential quadrature method," *Inter of Mechanical Science*, vol.49, Oct, 2006, pp. 447-453
- [9] Xinwei Wang, Lifei Gan and Yihui Zhang, "Differential quadrature analysis of the buckling of thin rectangular sheets with cosine-distributed compressive loads on two opposite sides," *Advances in Engineering Software*, vol.39, May, 2007, pp. 497-504
- [10] Seong-Min Kim, "Buckling and vibration of a sheet on elastic foundation subjected to in-plane compression and moving loads," *Inter Journal of Solids and Structures*, vol.41, Jun, 2004 pp.5647-5661
- [11] M. Eisenberger and A. Alexandrov, "Buckling loads of variable thickness thin isotropic sheets," *Thin-Walled Structures*, vol.41, Feb, 2003, pp.871-889
- [12] J. Rhodes, "Some observations on the post-buckling behaviour of thin sheets and thin-walled members," *Thin-Walled Structures*, vol.41 2003, pp.207-226
- [13] Le-Chung Shiau, Shih-Yao Kuo and Cheng-Yuan Chen, "Thermal buckling behavior of composite laminated sheets," *Composite Structures*, vol.92, Aug, 2009, pp.508-514
- [14] Hurang Hu, Ashraf Badir and Ayo Abatan, "Buckling behavior of a graphite/epoxy composite sheet under parabolic variation of axial loads," *Inter Journal of Mechanical Sciences*, vol.45, Aug, 2003, pp.1135-1147
- [15] M. Elgaaly, "Post-buckling behavior of thin steel sheets using computational models," *Advances in Engineering Software*, vol.31, 2000, pp.511-517
- [16] F. Guarracino, "Considerations on the numerical analysis of initial post-buckling behaviour in sheets and beams," *Thin-Walled Structures*, vol.45, Sep, 2007, pp.845-848
- [17] Mei-Wen Guo, Issam E. Harik and Wei-Xin Ren, "Buckling behavior of stiffened laminated sheets," *Inter Journal of Solids and Structures*, Vol.39, Feb, 2002, pp.3039-3055
- [18] H.R. Ovesy and H. Assae, "An investigation on the post-buckling behavior of symmetric cross-ply laminated sheets using a semi-energy finite strip approach," *Composite Structures*, vol.71, 2005, pp.365-370